Low Frequency Performance of Piezoelectric Accelerometer Nodes versus Geophone Arrays

Introduction

Land seismic acquisition in arid environments is typically constrained by complex heterogeneous near-surface conditions, limited source energy, and strong ambient noise. While high-frequency energy (≥ 30 Hz) provides fine lateral resolution, the low-frequency portion of the wavefield governs the ability to image deep structures and to construct robust velocity models (Ten Kroode et al., 2013). Recent advances in broadband source technology and sensor design (e.g., MEMS or piezoelectric accelerometers with flat response down to 1 Hz or lower) have boosted interest in quantifying the specific contributions of low frequency data to complex data analysis techniques such as Full Waveform Inversion (FWI) (Stopin et al., 2014).

While utilizing a dense grid of single-sensor broadband receivers would be an ideal case from the pure data quality point of view (Colombo et al., 2024, Goujon and O'Toole, 2024), it is still often more reasonable to rely on geophone or nodal arrays due to data size and acquisition logistics and economics. On modern nodal systems, digital group forming can be performed during the harvesting stage in real time (Ourabah, 2025), allowing the delivery of a data volume similar to the cabled array data (with better summation and improved bandwidth) while allowing future access to the sensor data via the continuous records.

In this paper, we provide a comprehensive comparison of the land seismic dataset recorded with 9-geophone arrays and co-located dense nodal acquisition with 9 single sensors combined using Digital Group Forming (DGF9) with a focus on low-frequency part of the spectra. We demonstrate that accelerometer data is superior in low frequency range and thus more suitable for FWI applications.

Method

We recorded field dataset with a static spread of ~16,000 single-sensor piezoelectric nodes. The nodes were deployed alongside a 3D production survey that used a 9-geophone cabled array per channel (3x3 array with 8.33m sensor spacing inline and crossline, 25m channel spacing inline). The geophones in the arrays have a natural frequency of 10Hz, which means the instrument response is flat only after 10Hz. On the other hand, the piezoelectric accelerometer nodes have a flat response between 1-125Hz, with a roll-off on both sides of the response.

The nodes were collocated with geophones along one receiver line to allow testing of various digital arrays during processing. As surface conditions allowed, all nodes were buried under a few centimetres of sand, in line with the manufacturer's recommendations. This burial provides insulation from external factors and leaves the surface unobstructed for source movement. Each group of nine traces recorded by nodes collocated with the 9-geophone array sensors were then combined using digital group forming DGF9 (Ourabah, 2025), thereby emulating the data output of the production cabled system.

The nodes were recorded continuously for approximately 14 days during vibroseis source acquisition, covering the full cross-line offset range of the main production survey. Source lines were oriented orthogonal to the receiver lines, spaced 100 m apart, with an inline station spacing of 25 m. The source geometry was designed for the production 3D survey, resulting in relatively sparse sampling for imaging when only a single receiver line is available for nodal data. Nevertheless, this geometry is sufficient for the objectives of this comparative study.

Results

Following the standard workflow, we applied the geophone inverse instrument filter to the velocity data recorded by the geophones, and we applied an integration and the inverse instrument filter of the nodes to the acceleration data recorded by the nodes. The comparison of the raw shot gathers recorded by geophone array and DGF9 is shown in Figure 1a and 1b, respectively. After accelerometer data integration and inverse instrument filters applied, both datasets look very similar (Figure 1c and 1d, respectively). However, closer look at the amplitude and phase spectra (Figure 1e and 1f) shows that accelerometer data is less attenuated in the lowest frequencies. Note that on Figure 1e, the normalization of the spectra is at 10Hz, which artificially elevates the amplitude of the raw geophone data (green curve) between 12 and 70 Hz, while this should be ~ 3 dB lower (as there is a ~3 dB attenuation at the natural frequency), bringing all curves to the same level between 20-60Hz.

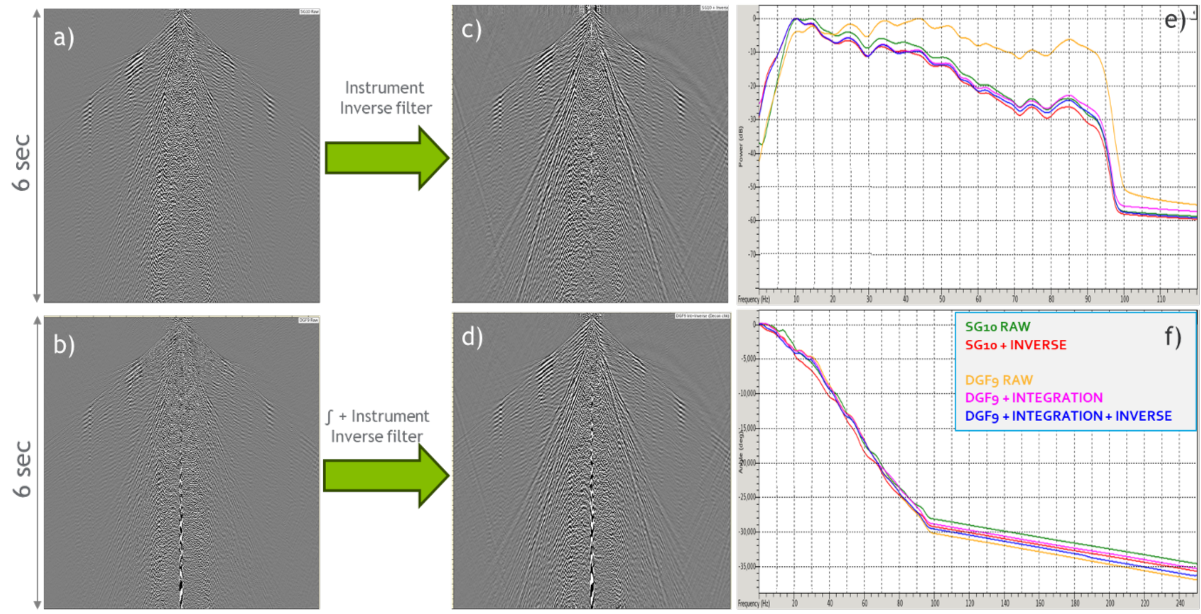

Figure 1. *Comparison of the raw records from 9-geophone array (a) and DGF9 (b). The geophone array response with instrument inverse filter applied is shown in (c) and DGF9 after integration to velocity and instrument inverse filter applied is shown in (d). Panels (e) and (f) demonstrate amplitude and phase spectra comparison, respectively (normalised plots).*

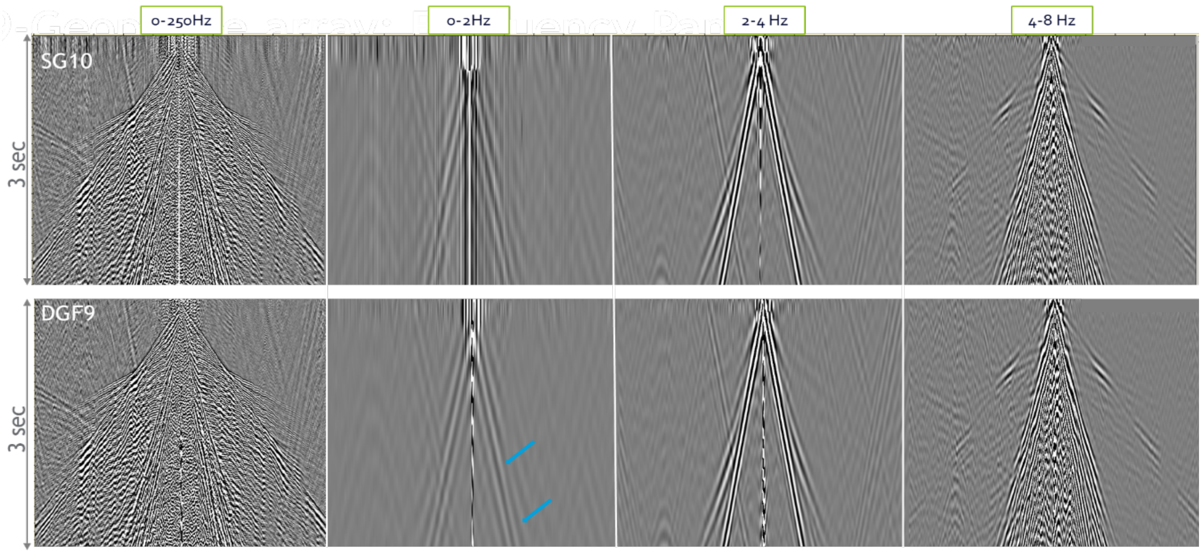

Figure 2. *Comparison between geophone array (top) and DGF9 (bottom) for the full bandwidth and narrow frequency ranges (all inverse filter applied respectively).*

Figure 2 provides a detailed comparison of the low-frequency content of the two datasets. The top row shows the geophone data, and the bottom row shows the node-based DGF9 data. The leftmost panels display the full-bandwidth data after application of the respective inverse sensor-response filters, while the remaining three columns show octave-band panels for 0-2 Hz, 2-4 Hz, and 4-8 Hz. The two datasets show very close agreement in the 2-8 Hz range, where the waveforms are nearly identical. In contrast, differences are observed in the lowest octave (0-2 Hz), where the signal, dominated by ground roll, is well preserved in the node's DGF9 data (highlighted by blue arrows) but appears distorted in the geophone array data. This behaviour may be attributed to variations in the individual geophone responses within the array (Tellier et al., 2021), which cannot be corrected for since the individual traces are summed at acquisition and are not retrievable.

Figure 3 compares both geophone array and node's DGF9 to the single-sensor (SS) nodal data with the focus on the far-offset refracted and reflected signal. The SS panel has 3 times more traces with the spatial sampling of 8.33m which results in unaliased surface wave recording (see FK-panels in lower-right corner). It is clear also from the amplitude spectra observation that the single sensor data delivers not only better high-frequency data but also an uplift in the low frequencies, an effect we will examine further in the next section.

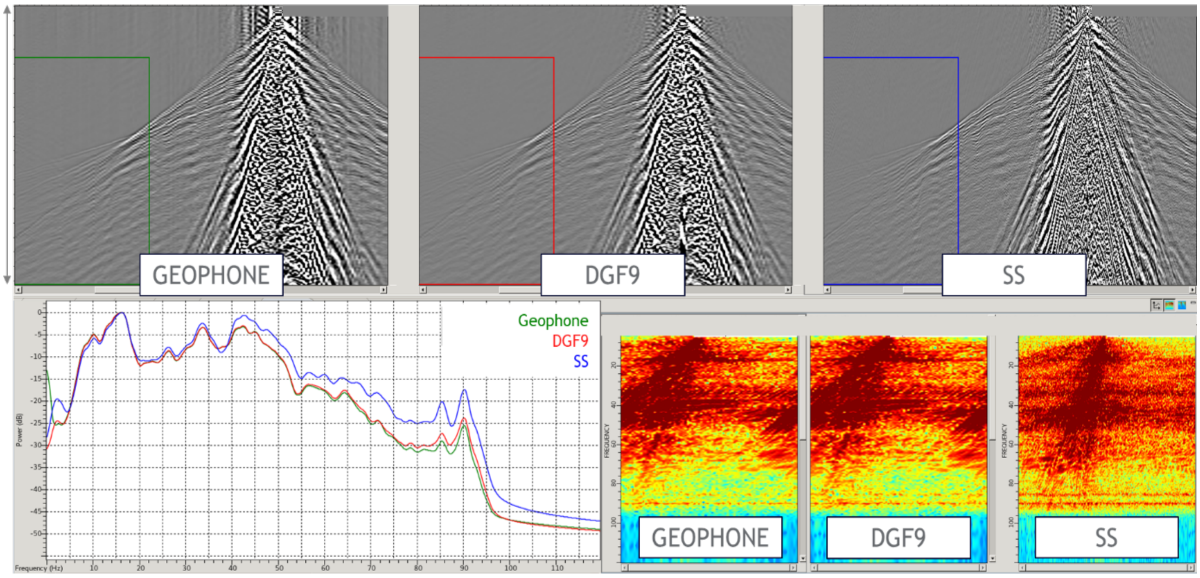

Figure 3. *Amplitude and FK spectra comparison for geophone array, DGF9 and single sensor nodal data with focus on far-offset refracted and reflected signal. The colour of the analysis frame corresponds to the colour of the amplitude spectrum line. (all inverse filter applied respectively).*

Considering orthogonal acquisition grids with different sampling intervals in the cross-line and inline directions for both sources and receivers, land-3D data are often analysed and processed in the cross-spread domain, where spatial sampling is equal in the two orthogonal directions. Figure 4 compares time slices for single sensor nodal data in full bandwidth (top) and the low-frequency (0-8 Hz) portion (bottom). The left column displays the raw recorded data while the right column shows data with dunes statics applied. We observe that dune statics are very prominent in the full-bandwidth data (illustrated by the rough circle of first arrivals) and when corrected, can significantly improve the wavefield coherency. This effect remains visible on the low-frequencies, which are still affected by these static shifts and show a much better phase alignment when statics are applied. This indicates that static corrections remain important for processes that uses low frequency data such as FWI, frequency-dependent velocity analysis, etc.

Conclusions

This study presents a comparison between a conventional geophone array and a digital array formed from nine individual traces recorded by piezoelectric accelerometers collocated with the geophones. The two datasets were acquired in a sand-dune environment with challenging surface conditions. Both array types show comparable performance across the recorded bandwidth, with raw data appearing nearly identical after correction for the respective sensor responses. At low frequencies, however, the DGF9 formed from piezoelectric accelerometer nodes provides improved performance, delivering cleaner signal in the 1-2 Hz range. We observed that the single sensor data recorded by the individual nodes also shows high performance across the full recorded bandwidth with a high spatial sampling that should significantly benefit data processing if data processed as single sensor, and offers the possibility to pre-process individual traces prior to summation if digital group forming is used, adding a flexibility that might be important for extending usable bandwidth and supporting full-waveform inversion applications.

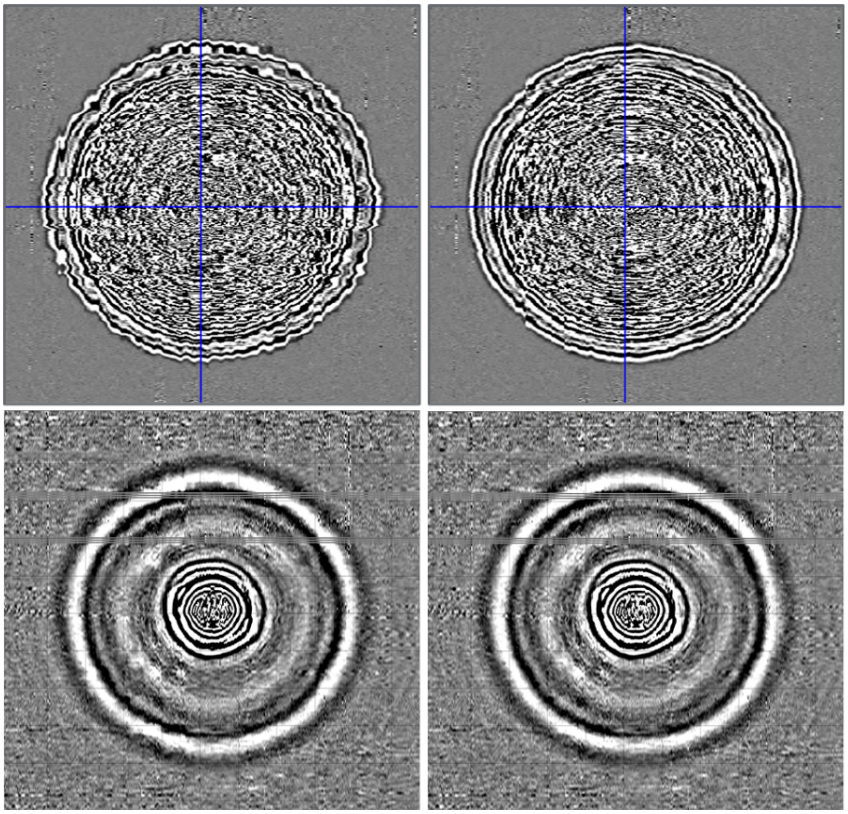

Figure 4. *A cross-spread time slice at 800ms of the single sensor data before dune statics (left) and after dune statics (right). Top displays use full frequency range; bottom displays show frequencies <8Hz only. The improvement of the wavefront coherency is clearly visible after static correction even at these low frequencies, highlighting the benefits of accessing the single sensor data for pre-processing to improve quality of low frequencies and phase stability.*

References

Colombo, D., E. Sandoval-Curiel, T. Alyousuf, E. Turkoglu, and D. Rovetta, 2024. Ultra-dense nodal seismic acquisition for automated geohazard analysis, The Leading Edge, 43(8), 484–492, https://doi.org/10.1190/tle43080484.1.

Goujon, N., and T. O'Toole, 2024. From geophone arrays to point receivers: Implications for sensor and land survey design: SEG Technical Program Expanded Abstracts, 297–301, https://doi.org/10.1190/image2024-4091851.1.

Ourabah, A., 2025. Processing on the edge: The evolution of in-field processing in modern land seismic surveys, First Break, 43(1), 69–73, https://doi.org/10.3997/1365-2397.fb2025006.

Stopin, A., Plessix, R.-E. and Said, A.A., 2014, Multiparameter waveform inversion of a large wide azimuth low-frequency land data set in Oman. Geophysics, 79(3), WA67–WA77.

Tellier, N., S. Laroche, H. Wang, and N. Tellier, 2021. Land Acquisition without Data Jitter Made Possible with MEMS Sensors, 82nd EAGE Annual Conference & Exhibition, European Association of Geoscientists & Engineers, 1–5, https://doi.org/10.3997/2214-4609.202112510

Ten Kroode, A. P. E., Bergler, S., Corsten, C., de Maag, J. W., Strijbos, F. and Tijhof, H., 2013, Broadband seismic data. The importance of low frequencies. Geophysics, 78(2), WA3–WA14, doi:10.1190/geo2012-0294.1.